ACI MATERIALS JOURNAL TECHNICAL PAPER

Title No. 120-M46

Pozzolanic Reactivity of Supplementary Cementitious Materials

by Keshav Bharadwaj, O. Burkan Isgor, and W. Jason Weiss

As the number of potential supplementary cementitious materials (SCMs) increase, there is a need to determine their reactivity. Most recent methods to assess pozzolanic reactivity are based on measuring certain outputs such as heat release (Q), calcium hydroxide (CH) consumption, and nonevaporable water. This paper uses thermodynamic modeling to aid in the interpretation of these tests and the quantification of reactivity. It is shown that pozzolanic reactivity should be interpreted based on the SCM type. The presence of sulfates and carbonates during reactivity quantification alter the reaction of the Al_2O_3 phases, making the interpretation of the reactivity test results challenging. The reactivity of commercial SCMs should be interpreted specific to the type of SCM as described by ASTM International/AASHTO. A proposed interpretation for commercial SCMs is provided in this paper.

Keywords: pozzolanic reactivity test (PRT); reactivity; supplementary cementitious materials (SCMs); thermodynamic modeling.

INTRODUCTION

The concrete industry has been actively working toward reducing the carbon footprint of concrete. One approach that is widely used to reduce the carbon footprint is to replace a portion of the ordinary portland cement (OPC) in concrete with supplementary cementitious materials (SCMs), which can also improve the performance of concrete. For example, the replacement of OPC with SCMs such as fly ash and silica fume in concrete have been shown to improve compressive strength,[1,2] reduce transport of deleterious ions by refining the pore structure,[1-5] control alkali-silica reaction (ASR) damage,[6,7] and mitigate the potential for calcium oxychloride formation and damage.[8-11] While questions exist regarding the future availability of some SCMs such as fly ash, partly due to the closure of coal combustion plants,[12] there are several other new sources for SCMs such as harvested ashes, agricultural/forest waste ash, municipal waste ash, and natural pozzolans that may be used in concrete.[12-19] However, there is a need for tests to screen and evaluate the performance of SCMs obtained from the new or modified sources for their appropriate use in concrete.[20]

The performance of concrete containing SCMs depends on the: 1) chemical and physical composition of the SCM[21,22]; 2) the reactivity of the SCM (that is, fraction of the phases in the SCM that can react)[1,23]; and 3) the kinetics of reaction of these phases.[24] Standards such as ASTM C618[25] or AASHTO M 295[26] (in the case of fly ash and natural pozzolans) specify the compositional and physical requirements for SCMs, but they do not provide a reliable method to assess how reactive these materials are. Over the years, various approaches have been used to try to ascertain the amount of SCM that can replace OPC, such as by predicting strengths using k-factors.[27,28] These empirical factors were used as a surrogate for the SCM reactivity. Some researchers have assumed the amorphous content as the reactive component of SCM.[29,30] Over the years, several test methods were developed to directly measure reactivity of SCMs for their use in concrete. Some of these are relatively old (for example, the Frattini test[31] or the Chapelle test[32]) and have documented limitations.[33-35] Newer methods to assess pozzolanic reactivity such as the ASTM C1987 test[36] (also known as the "R3 test"[37,38]) and the pozzolanic reactivity test (PRT)[23,33,39] are based on measuring certain outputs of the test to provide a better understanding of SCM reactivity. For example, the primary output of the R3 test is the weight of bound water when heated up to 400°C or the ultimate heat released, which can be used to provide a relative reactivity to compare SCMs of the same type. The outputs of the PRT are heat release (Q) and calcium hydroxide (CH) consumption, which are then used to obtain a numerical value of maximum degree of reactivity (DOR*) of an SCM.[39] The DOR* can also be used as an input to perform thermodynamic calculations and can be used to predict concrete properties for assessing performance.[3,20,40-45] The DOR* serves as a key parameter for performance-based concrete mixture design.[20]

In recent years, the use of Q and CH consumption as an indicator for pozzolanic reactivity has been extensively studied using experimental investigations.[3,23,29,33,37,39,41,46-60] It can be noted that examining these values as a function of time can provide information on the kinetics of SCM reactions. However, these experimental studies are limited by the types, chemical compositions, and reactivities of tested SCMs; therefore, it is not always possible to generalize their conclusions. Thermodynamic modeling of cementitious systems has been a powerful tool that can aid in interpreting experimental studies and has been shown to provide supporting insight to experiments. In this paper, the authors use thermodynamic modeling to explore various aspects of pozzolanic reactivity of SCMs.

The first question that this paper addresses is if the pozzolanic reactivity should be measured and/or interpreted differently for different types of SCMs. For example, in the present form, the PRT quantifies the reactivity of SCMs

ACI Materials Journal, V. 120, No. 4, July 2023.

MS No. M-2022-277.R1, doi: 10.14359/51738817, received August 26, 2022, and reviewed under Institute publication policies.

(DOR*) by comparing the measured Q and CH consumption with the theoretical values of Q and CH consumed by pure SiO_2 and pure Al_2O_3 at various degrees of reaction. This approach implies that the DOR* of siliceous materials such as silica fume and fly ash can be quantified accurately. However, the applicability of this approach to quantify the DOR* of silico-aluminous SCMs (for example, calcined clays) or those showing hydraulic properties (for example, slag) needs further investigation. Silico-aluminous SCMs contain comparable portions of silica and alumina, and alumina reactions could affect the interpretation of the Q and CH consumption output.[39] Hydraulic SCMs typically contain the reactions of CaO in the system, which affect the measured Q and CH consumption, while these reactions are not considered pozzolanic in nature. Therefore, in this paper, the effect of SCM type on the measurement and interpretation of pozzolanic reactivity is explored. The second question that this paper addresses is if the presence of sulfates and carbonates in the system affect the measurement and/or interpretation of the pozzolanic reactivity of SCMs. It is clear that the presence of sulfates and carbonates would induce additional reactions in the cementitious mixture, but whether or not these reactions should be considered as part of the measurement and interpretation of pozzolanic reactivity of SCMs need to be investigated further.

These questions are answered though the thermodynamic modeling of the PRT using various SCMs in different chemical conditions. The PRT is selected as a test method because it provided a numerical value of pozzolanic reactivity (that is, DOR*), and the measured outputs in the PRT (that is, Q and CH consumption) could be modeled through thermodynamic modeling. First, ideal SCMs comprising of only a combination of SiO_2 and Al_2O_3 were studied. The SiO_2:Al_2O_3 in the SCM is varied and the phases that form in the PRT (reaction products), Q, and CH consumed are examined. This investigation is intended to understand the interpretation of the reactivity of aluminous SCMs more accurately. Second, ideal SCMs that are combinations of SiO_2, Al_2O_3, and CaO were studied. The influence of CaO on the reaction products, Q, and CH consumed is examined. This investigation is intended to understand the interpretation of the reactivity of SCMs that show hydraulic properties better. Third, it was studied whether the presence of sulfates and carbonates affect the interpretation of the reactivity of SCMs containing SiO_2, Al_2O_3, and CaO. Finally, the first three modeling studies to commercially available SCMs with typical chemistries were expanded. The knowledge generated in this study allows for a more accurate quantification of the SCM reactivity, which can be used to improve the performance of concrete by allowing for the selection of the appropriate SCMs for use in concrete.[20]

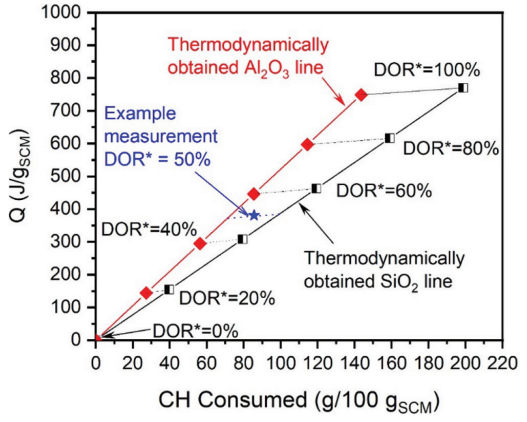

Fig. 1—Example schematic presentation of results of PRT on Q-CH consumed plot showing example experimental measurement, theoretical lines for pure SiO_2 and pure Al_2O_3, and interpolation to calculate DOR from experimental measurement.*

RESEARCH SIGNIFICANCE

This paper uses thermodynamic modeling to aid the interpretation of pozzolanic reactivity testing of SCMs. The study answers two key questions: 1) should the pozzolanic reactivity measured and/or interpreted differently for different types of SCMs based on the reaction products that form; and 2) does the presence of sulfates and/or carbonates in the system affect the measurement and/or interpretation of the pozzolanic reactivity of SCMs? The paper also makes recommendations to quantify the pozzolanic reactivity of commercial SCMs.

METHODS

Pozzolanic reactivity test (PRT) method

The PRT is a method to determine the DOR* of an SCM. The PRT is performed by reacting the SCM with an excess of CH (3:1 CH:SCM by mass) and an excess of an alkaline pore solution (0.5 N KOH solution; liquid-to-(CH+SCM) ratio is 0.90 by mass) at 50°C for 240 hours.[23,33] The test measures the Q of the reaction using an isothermal calorimeter (IC) and the CH consumed by the reaction using a thermogravimetric analyzer (TGA). For this test, only small amounts of the SCM are needed. In the standard procedure, 40 g of SCM is mixed with 120 g of CH and 144 g of 0.5 N KOH solution. Approximately 7 g of the paste is sealed in a glass ampule and loaded into the IC and the heat released is recorded for 240 hours. At the end of the 240 hours, approximately 20 mg of the reacted paste is loaded onto a platinum crucible of the TGA and the mass of CH remaining after the reaction is determined using the TGA using the approach developed by Kim and Olek.[61] The CH consumed is calculated as the difference between the initial mass of CH and the CH remaining after the reaction. In the PRT, the experimentally measured values of Q and CH consumed are plotted in the Q-CH consumed space. The theoretical Q and CH consumed of pure SiO_2 and pure Al_2O_3 are calculated using thermodynamic data and plotted as lines on the same plot. The value of DOR* is calculated by interpolating the experimental results between the theoretical SiO_2 and Al_2O_3 lines. Figure 1 is an illustration of the PRT showing an example measurement from an experiment, the theoretical lines obtained for pure SiO_2 and pure Al_2O_3, and the interpolation to obtain the DOR* of the SCM. The DOR* can also be quantified in the PRT using Eq. (1)[33]

$$DOR^* = a_1 Q + a_2 CH_{consumed} \quad (1)$$

where Q is measured in J/gSCM; $CH_{consumed}$ is measured in g/100g SCM; and a_1 and a_2 are constants (for the PRT, $a_1 = 1.44 \times 10^{-3}$/(J/$g_{SCM}$) and $a_2 = -0.54 \times 10^{-3}$/(g/100$g_{SCM}$), obtained from Reference 33).

Thermodynamic modeling

In this work, thermodynamic modeling is used to better interpret the PRT results by calculating the volume and compositions of the reaction products that form in the PRT as well as heat release during these reactions.[23,33,62,63] The calculations are done using GEMS3K[64] software in conjunction with the CemData v18.01[65] and PSI/Nagra[64] databases, which performs thermodynamic calculations by minimizing the Gibbs free energy of the reaction products for a given set of inputs compositions, and are used in conjunction with GEMS3K for the calculation of reaction products of cementitious systems. While all possible reaction products in cementitious systems are available in the CemData v18.01 database, the formation of some phases is blocked based on evidence from the literature that these phases do not form in significant quantities in the PRT.[65,66] The blocked phases are C_3AH_6,[66,67] Gibbsite,[65] and some AFm phases (C_4AH_{13}, C_4AH_{19}, C_4AsH_{12}). The Q is calculated by subtracting the total enthalpies of the reaction inputs from the total enthalpies of the reaction products, which are obtained from CemData v18.01 database[65] and the NIST Chemistry WebBook.[68]

RESULTS AND DISCUSSIONS

Ideal SCMs containing only SiO_2 and Al_2O_3

This section examines the phases that form, and the theoretical values of Q and CH consumed, when the proportions of SiO_2 and Al_2O_3 are varied when PRT is used to test an SCM containing only SiO_2 and Al_2O_3. Figure 2(a) shows the phases that form as the proportion of SiO_2 and Al_2O_3 is varied in an SCM that is 100% reactive when tested in the PRT. When the SCM contains only Al_2O_3, all alumina reacts to form $C_2AH_{7.5}$, releasing 748J/g_{SCM} heat and consuming 144 g of CH per 100 g SCM. As the proportion of silica in the SCM increases from 0% by weight to 36.65%, the silica and alumina preferentially react to form C_2ASH_8, and the remaining alumina (if any) reacts with the CH to form $C_2AH_{7.5}$. While it is generally considered that C_2ASH_8 and CH cannot coexist in the same system, the formation of C_2ASH_8 has been reported in experiments[69] in metakaolin+CH systems, in line with the model predictions. The Q decreases from 748 J/g_{SCM} (for 100% Al_2O_3) to 647 J/g_{SCM} (for 63.35% Al_2O_3 + 36.65% SiO_2). The CH consumed reduces from 144 g/100 g_{SCM} (for pure alumina) to 90 g/100 g_{SCM} (for 63.35% Al_2O_3 + 36.65% SiO_2). The

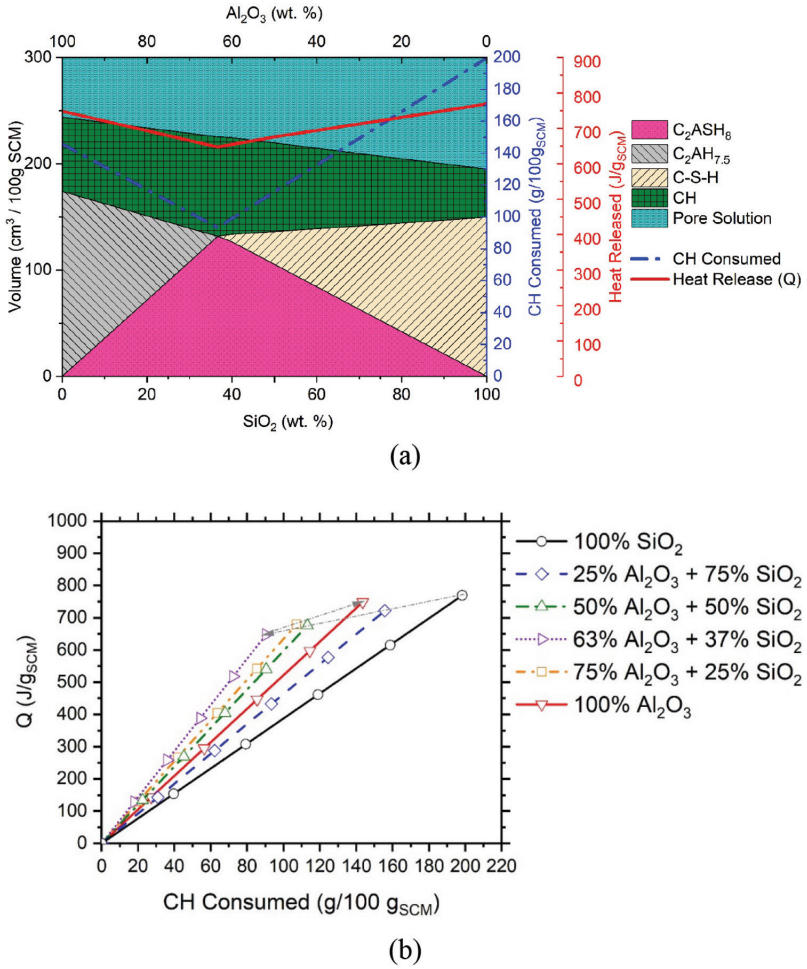

Fig. 2—(a) Phases that form as proportion of SiO_2 to Al_2O_3 is varied; and (b) reactivity lines: values of Q versus CH consumed for ideal SCMs containing varying proportions of SiO_2 and Al_2O_3.

Table 1—Reactions in PRT and their corresponding Q and CH consumed

Reaction No.	Reaction in PRT	Q, J/g_{SCM}
1	100 g SiO_2 + 198 g CH + H_2O → C-S-H	769
2	100 g Al_2O_3 + 144 g CH + H_2O → $C_2AH_{7.5}$	748
3	100 g (Al_2O_3 + SiO_2) + 90 g CH + H_2O → C_2ASH_8 (SiO_2: Al_2O_3 = 0.58 by wt.)	647
4	100g CaO + H_2O → CH	1149
5	100 g Al_2O_3 + 167 g gypsum + 215 g CH + H_2O → monosulfate	1244
6	100 g Al_2O_3 + 49 g $CaCO_3$ + 254 g CH + H_2O → hemicarbonate	1291
7	100 g Al_2O_3 + 98 g $CaCO_3$ + 218 g CH + H_2O → monocarbonate	1402

"critical composition" of 63.35% Al_2O_3+36.65% SiO_2 (when SiO_2:Al_2O_3 = 0.58) represents the minimum of Q and the minimum CH consumed for an SCM consisting of only SiO_2 and Al_2O_3 tested in the PRT, as C_2ASH_8 is the only phase formed. As the SiO_2 in the SCM increases from 36.65% to 100%, C_2ASH_8 + C-S-H forms. The Q increases from 647 J/g_{SCM} (for 63.35% Al_2O_3 + 36.65% SiO_2) to 769 J/g_{SCM} (for pure silica). The CH consumed increases from 90 g/100 g_{SCM} (for 63.35% Al_2O_3 + 36.65% SiO_2) to 198 g/100 g_{SCM} (for pure silica). The Q and CH consumed by the reactions in the PRT is summarized in Table 1. The composition of the C-S-H that is predicted to form in the PRT is uniform (C/S = 1.7), irrespective of the silica content in the SCM, as there is an excess of CH in the system. The impact of the C-S-H model used (CSHQ versus CNASH) is shown in Appendix A*; briefly, the CSHQ model is sufficient for calculating the DOR* of the SCM using the PRT.

Figure 2(b) shows the theoretical values of the Q versus the CH consumed for varying levels of reactivity for an SCM made with varying proportions of SiO_2 and Al_2O_3 plotted on the PRT-style plot. The term "reactivity line" refers to the line obtained by plotting the Q versus CH consumed obtained from thermodynamic calculations of the SCM composition. The SiO_2 reactivity line (line for an SCM made on only silica; black solid line with circle markers in Fig. 2(b)) is the rightmost line on the plot as the reaction of pure silica to form C-S-H results in the highest Q and highest CH consumed. As the mass fraction of alumina in the SCM is increased from 0 to 63.35%, the reactivity line shifts to the left (as shown in the figure with an arrow) due to a decrease in the CH consumed, and the length of the line decreases as the Q and CH consumed decrease as C_2ASH_8 forms at the expense of C-S-H. As the alumina content in the SCM is increased from 63.35 to 100% (pure alumina), the line shifts to the right (as shown in the figure with an arrow) due to an increase in the CH consumed, and the length of the line increases as the Q and CH consumed increase. The Al_2O_3 reactivity line (line for an SCM containing only alumina; red solid line with triangle markers in Fig. 2(b)) is still to the left of the SiO_2 reactivity line, as the CH consumed by the reaction of pure alumina is lower than the CH consumed by the reaction of pure silica.

The results shown in Fig. 2(b) offer insight into the typical behavior of SCMs, which do not contain significant CaO (for example, silica fume, Class F fly ashes, metakaolin calcined clays, and natural pozzolans such as pumice) in the PRT. Silica fume, which typically contains more than 85% SiO_2,[55,70,71] is expected to appear in the rightmost end of this plot as the reaction of silica to form C-S-H consumes the most CH and releases the most heat. Class F fly ashes or natural pozzolans, which typically contain 45 to 55% SiO_2 and 19 to 25% Al_2O_3,[40,55] would fall between the SiO_2 line and the 75% SiO_2 + 25% Al_2O_3 line. Metakaolin and calcined clays, which typically contain 50 to 60% SiO_2 and 30 to 45% Al_2O_3,[55] would fall on or around the 50% SiO_2 + 50% Al_2O_3 line.

Ideal SCMs containing SiO_2, Al_2O_3, and CaO

This section examines the phases that form Q and CH consumed in PRT when the proportions of CaO, SiO_2, and Al_2O_3 are varied in an ideal SCM containing only pure CaO, SiO_2, and Al_2O_3. Thermodynamic calculations predict that the reaction of CaO can be decoupled from the reaction of SiO_2 and Al_2O_3. The CaO (from the SCM) reacts with water to form CH (which is a hydraulic reaction), which can further react with the SiO_2 and Al_2O_3 to form C-S-H, C_2ASH_8, and $C_2AH_{7.5}$ depending on the SiO_2:Al_2O_3 in the SCM. Figure 3 shows the phase assemblage of an SCM containing 25% CaO with varying SiO_2 to Al_2O_3 masses. When the SCM contains only Al_2O_3 (no SiO_2), $C_2AH_{7.5}$ forms. As the mass of SiO_2 in the SCM increases from 0 to 27.5% in the SCM (the SiO_2:Al_2O_3 changes from 0 to 0.58), C_2ASH_8 forms along with $C_2AH_{7.5}$. This is associated with a corresponding decrease in Q and CH consumed. As the SiO_2 mass in the SCM increases from 27.5 to 75% (note that CaO = 25%, so the highest mass of SiO_2 in the SCM can be 75%), C-S-H phases form along with C_2ASH_8, which is associated with an increase in Q and CH consumed. The minimum of Q and CH consumed still occurs at a critical ratio of SiO_2 to Al_2O_3 in the SCM (SiO_2:Al_2O_3 = 0.58), and this value appears to be constant irrespective of the CaO content of the SCM. This is because the reaction of the SCM in the PRT when the SiO_2:Al_2O_3 = 0.58 forms only C_2ASH_8.

Figure 4(a) shows the phase assemblage of an SCM containing only SiO_2 and CaO, with an increasing CaO content. As the CaO content increases, the amount of CH in the system increases due to the reaction of CaO with water to produce CH. As the proportion of CaO in the SCM increases, the amount of SiO_2 in the SCM decreases

*The Appendix is available at **www.concrete.org/publications** in PDF format, appended to the online version of the published paper. It is also available in hard copy from ACI headquarters for a fee equal to the cost of reproduction plus handling at the time of the request.

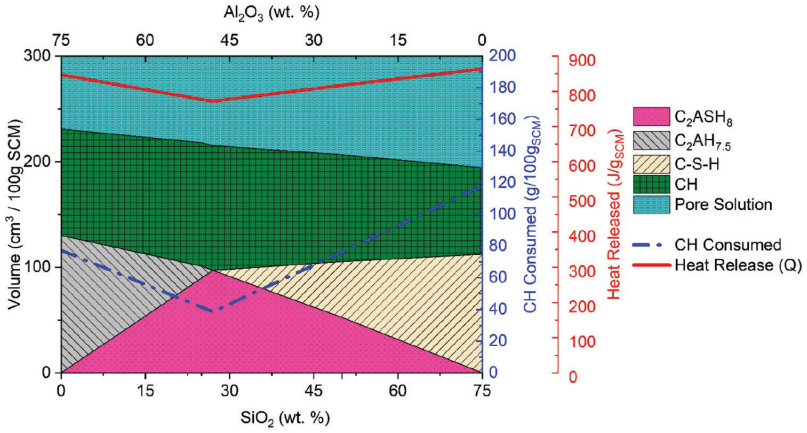

Fig. 3—Plot of phase assemblage for SCM containing 25% CaO with SiO_2:Al_2O_3 varying.

(because SiO_2 = 100% – CaO in this SCM), and the following are observed: 1) volume of C-S-H that forms at equilibrium decreases; 2) the Q increases as the reaction of CaO produces more heat than the reaction of SiO_2 in the PRT (refer to Table 1); and 3) the CH in the system increases due to the hydraulic reaction of CaO to form CH, which translates to a net reduction in CH consumed.

Figure 4(b) shows the phase assemblage of an SCM containing only Al_2O_3 and CaO, with an increasing CaO content. As the CaO content increases: 1) the volume of $C_2AH_{7.5}$ that forms decreases, as there is a lesser proportion of Al_2O_3; 2) the Q increases (the reaction of CaO that produces CH releases 401 J/g SCM more heat than the reaction of Al_2O_3 to form $C_2AH_{7.5}$; refer to Table 1); and 3) the CH in the system increases and there is a net reduction in CH consumed.

Figure 4(c) shows the phase assemblage of an SCM containing the critical mass ratio of SiO_2:Al_2O_3 = 0.58 and CaO, with an increasing CaO content. As the CaO content increases: 1) the volume of C_2ASH_8 that forms decreases due to the reduction in the amount of SiO_2+Al_2O_3 in the SCM; 2) the Q increases; and 3) the CH in the system increases due to this reaction. The Q and CH consumed by each reaction in the PRT is summarized in Table 1. Note that the Q is the cumulative heat released at complete reaction for the particular composition of SCM simulated.

Figure 5 shows a plot of how the reactivity lines vary when CaO is present in the SCM. SCMs containing 0, 25, 50, 75, and 100% wt. % CaO are shown. At each CaO content, three lines are shown: the remaining mass of SCM is SiO_2 (black solid line), the remaining mass of SCM is Al_2O_3 (red dashed line), and the remaining mass of the SCM is SiO_2 + Al_2O_3 in the critical mass ratio of SiO_2:Al_2O_3 = 0.58 (green dash-dot line) (full-color PDF can be accessed at www.concrete.org). As the CaO content of the SCM increases, the heights of all three lines increase (due to an increase in the Q) and the lines move to the left (a decrease in the CH consumed). This is because the reaction of CaO in the PRT produces more heat than the reaction of SiO_2, Al_2O_3, or a combination of SiO_2 and Al_2O_3 in the PRT. The reaction of CaO also causes a decrease in the CH consumed as the reaction of CaO results in the production of CH. This behavior is well corroborated by experiments,[55] where it is seen that SCMs containing a significant amount of CaO such as slag release 400 to 600 J/g_{SCM} heat but consume only 20 to 60 g CH/100 g SCM. Note from Fig. 5 that the Q and CH consumed follow a linear behavior with respect to the CaO fraction in the SCM, which was seen in Fig. 4. If a line were to be drawn at any DOR* value (although only the 100% DOR* points are connected in Fig. 5), the Q and CH consumed plot follows a straight line from the 100% CaO to the 100% SiO_2 (thin dashed black line), 100% CaO to 100% Al_2O_3 (thin dotted red line), 100% CaO to 100% (SiO_2 + Al_2O_3) (thin dash-dot-dot green line) reactivity lines.

The practical implications of this finding are that it expands the scope of the PRT to determine the DOR* of hydraulic SCMs (such as slag) as well as pozzolans. Because the CaO reactions produce more heat than the reactions of SiO_2 and Al_2O_3 in the PRT, the reactivity lines used need to be revised when SCMs contain a significant amount of CaO. For example, slags typically contain 30 to 50% CaO, which means the Q measured in the PRT for slags will be 90 to 120 J/g SCM higher than pozzolanic SCMs such as silica fume and metakaolin for a 60% DOR*. The CH consumed by the slag of 60% reactivity would also be 40 to 80 g/100 g SCM lower than the silica fume or metakaolin of the same reactivity. If the appropriate CaO containing reactivity line is not used to determine the DOR*, and the pure SiO_2 and Al_2O_3 lines are used to determine DOR*, the reactivity would be erroneously determined to be 15 to 20% higher. Therefore, one should be careful while interpreting the Q and CH consumed from the PRT to measure the DOR* when the SCM contains CaO. This is explained later in this paper.

Influence of addition of sulfates and carbonates to pore solution

There is a debate in the literature on whether sulfates and carbonates should be added to tests when measuring the pozzolanic reactivity of SCMs.[33,37,38] The R3 test proposes the addition of sulfates and carbonates in an effort to mimic the pore solution chemistry of concrete,[37,38] while the PRT does not add sulfates and carbonates to measure only the Q and CH associated with the pozzolanic reaction.[33] This section of this paper aims to provide an insight into the changes to the reactions, Q, and CH consumed for SCMs of different chemistry when sulfates and carbonates are added

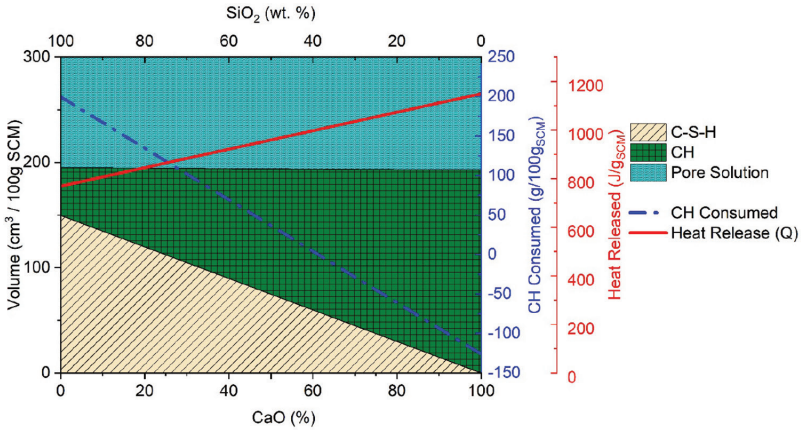

(a)

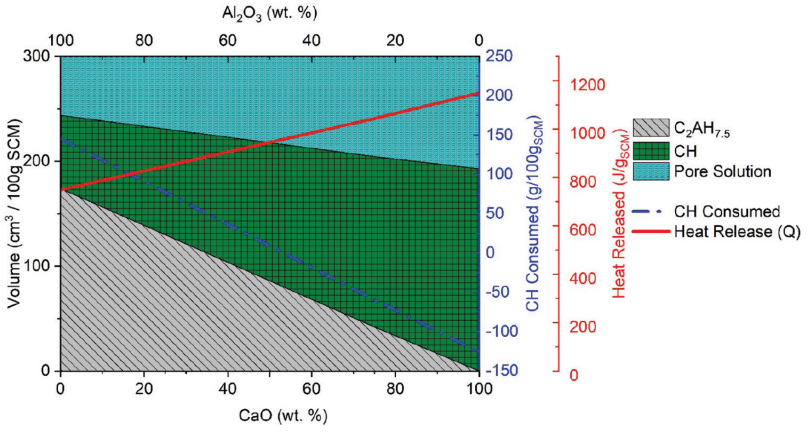

(b)

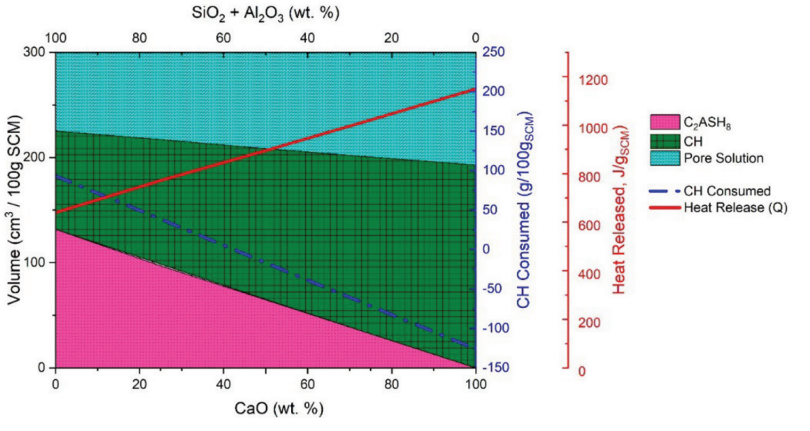

(c)

Fig. 4—Plot of phase assemblage, Q, and CH consumed for: (a) SCM containing only SiO_2 and CaO (no Al_2O_3), SiO_2:CaO varying; (b) SCM containing only Al_2O_3 and CaO (no SiO_2), Al_2O_3:CaO varying; and (c) SCM containing critical mass ratio of SiO_2:Al_2O_3 = 0.58, (SiO_2 + Al_2O_3):CaO varying.

to the pore solution in the PRT. Choudhary et al.[33] showed that the SiO_2 in the SCM does not react with the sulfates or carbonates, and the Al_2O_3 in the SCM reacts with the sulfates to form monosulfates and with carbonates to form carboaluminates preferentially at the expense of $C_2AH_{7.5}$ and C_2ASH_8. When both sulfates and carbonates are present, the compounds that form in the PRT can be a combination of monosulfate, carboaluminates, ettringite, C_2ASH_8, C-S-H, and $C_2AH_{7.5}$ phases depending on the molar ratio of sulfate to carbonate to alumina in the system[72] and the ratio of SiO_2 to Al_2O_3 in the SCM.

Figure 6(a) shows the phase assemblage of an SCM containing only SiO_2 and Al_2O_3 tested in the PRT when sulfates are added (as an example, 20 g gypsum/100 g_{SCM} addition is shown). When 100% Al_2O_3 is tested in the PRT, the Al_2O_3 preferentially reacts with the sulfates to

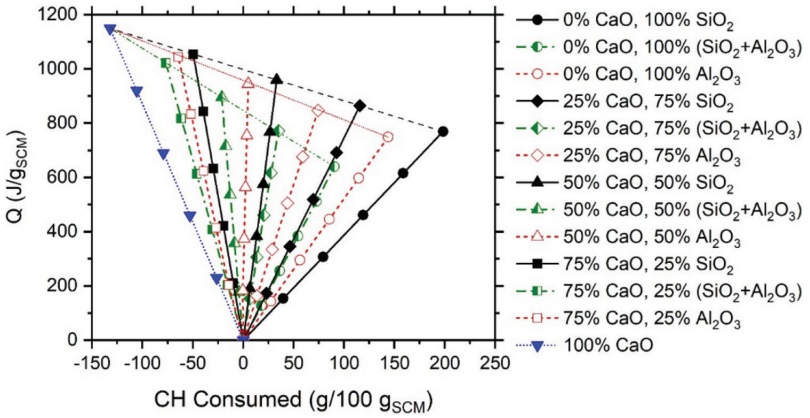

Fig. 5—Plot of Q versus CH consumed when SCMs of varying compositions are subject to PRT.

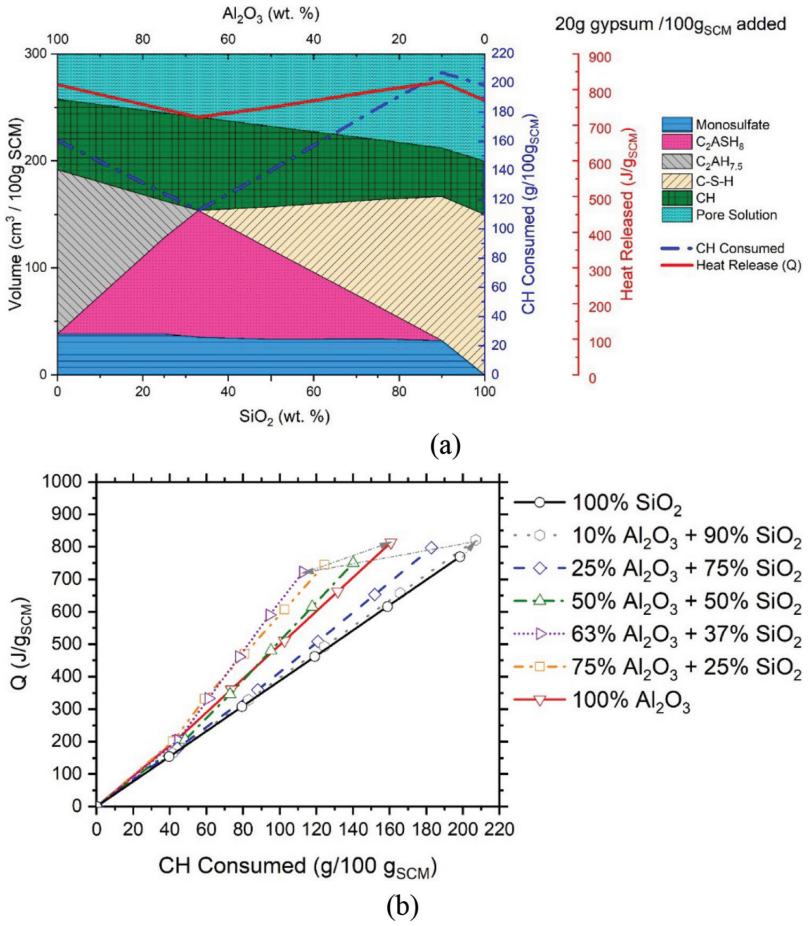

Fig. 6—(a) Plot of phases formed, Q, and CH consumed when sulfates are added to SCMs of varying compositions are subject to PRT; and (b) plot of Q versus CH consumed when SCMs of varying compositions are subject to PRT and 20 g gypsum is added.

produce monosulfates, and any remaining alumina (alumina remaining after all the sulfates are consumed) reacts pozzolanically to form $C_2AH_{7.5}$. The Q and CH consumed by alumina are higher when sulfates are present due to the formation of monosulfate.[33] As the amount of SiO_2 in the SCM increases from 0 to 33%, C_2ASH_8 forms in addition to the monosulfates and $C_2AH_{7.5}$. The volume of monosulfate formed is relatively constant as the alumina preferentially reacts with the sulfate, and only the remaining alumina reacts to form $C_2AH_{7.5}$ and C_2ASH_8. The Q and CH consumed also drop from 813 J/g_{SCM} and 161 g/100 g_{SCM} to 722 J/g_{SCM} and 113 g/100 g_{SCM}, respectively, due to the formation of C_2ASH_8. The Q and CH consumed by the sulfate reaction with Al_2O_3 in the PRT is summarized in Table 1. It can also be seen that the critical point of SiO_2 + Al_2O_3 has changed from 36% SiO_2 + 64% Al_2O_3 (in a system without sulfate) to 33% SiO_2 + 67% Al_2O_3 as some of the alumina is preferentially bound in the monosulfate, and only the remaining alumina in the SCM can react with SiO_2 and CH to form C_2ASH_8. As the SiO_2 is increased from 33 to 90%, C-S-H

phases form in addition to C_2ASH_8 and monosulfate. This causes an increase in the Q and CH consumed. Above a 90% SiO_2 content, all the alumina is bound in the monosulfate and there is no alumina available to react with the SiO_2 to form C_2ASH_8, so only C-S-H and monosulfate form. When the SCM is 100% SiO_2, only C-S-H forms.

The practical implications of this finding are that if sulfates are added during the measurement of reactivity, the reactions that form monosulfate need to be accounted for while determining the reactivity of the SCM using the heat released and CH consumed.[33] This can be done by determining the amount of alumina from the SCM that reacts with the sulfates. Figure 6(b) shows an example of the modification to the reactivity lines made for varying SiO_2:Al_2O_3 ratios in an SCM when 20 g gypsum/100 g SCM is added in the PRT. As expected, the 100% SiO_2 line is unaffected by the presence of sulfates. As the alumina content of the SCM increases, the top of the lines (100% DOR* point in each line) moves in the same manner as explained in the previous paragraph as shown using the arrow (Q and CH consumed increase with an increase in the sulfate added) as shown in Fig. 6(a). Some reactivity lines have kinks/bends on them. This is due to the preferential reaction of alumina with sulfate to form monosulfate, which has a higher Q/CH consumed (which is the "slope" of the line) than $C_2AH_{7.5}$. The location of the kink on a line of given composition is the point at which the reactive alumina exceeds the amount of alumina that can be consumed in the reaction that produces monosulfate—that is, for DOR* values below the kink in the line, only monosulfate forms; for the DOR* values above the kink in the line, monosulfate and $C_2AH_{7.5}$ + C_2ASH_8 form. As such, most commercial SCMs contain high levels of silica and low levels of alumina, which can pose a challenge while measuring the reactivity using the R3 test when sulfates are present due to the varying amounts of monosulfates that can form. Therefore, the addition of sulfates is not recommended while measuring the reactivity of SCMs.

Figure 7(a) shows the phase assemblage of an SCM containing only SiO_2 and Al_2O_3 tested in the PRT when carbonates are added (for illustration purposes, 5 g $CaCO_3$/100 g_{SCM} is added). Similar to sulfates, when Al_2O_3 is present in the SCM, the Al_2O_3 preferentially reacts with the carbonates to produce carboaluminates, and the remaining alumina (alumina remaining after all the carbonates are consumed) reacts pozzolanically to form $C_2AH_{7.5}$/C_2ASH_8. The Q and CH consumed by pure alumina is higher when

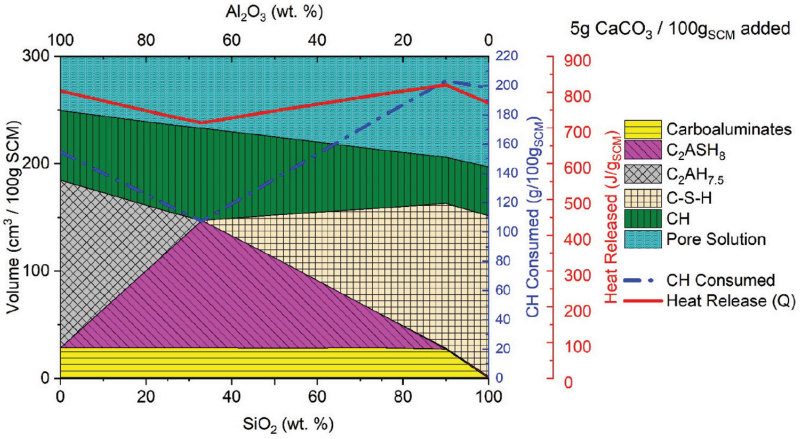

(a) Influence of carbonates on the varying SiO_2:Al_2O_3 in the SCM

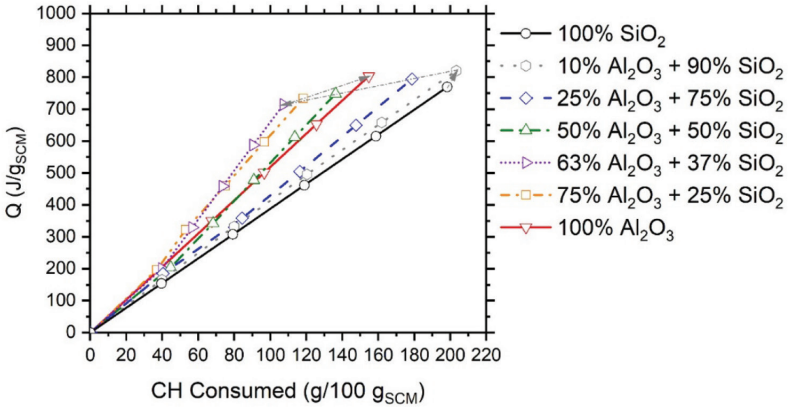

(b) Plot of the heat release and CH consumed when SCMs of varying compositions are subject to the PRT and 5g $CaCO_3$ is added

Fig. 7—(a) Plot of phases formed, Q, and CH consumed when carbonates are added to SCMs of varying compositions are subject to PRT; and (b) plot of Q versus CH consumed when SCMs of varying compositions are subject to PRT and 5 g $CaCO_3$ is added.

carbonates are present due to the formation of carboaluminates.[33] When the SCM is 100% Al_2O_3, carboaluminates + $C_2AH_{7.5}$ form. As the wt. % SiO_2 in the SCM increases from 0% to 33%, C_2ASH_8 forms in addition to the carboaluminates and $C_2AH_{7.5}$. The volume of carboaluminates formed as the SiO_2:Al_2O_3 of the SCM is varied is relatively constant as the alumina preferentially reacts with the carbonate, and only the remaining alumina reacts to form $C_2AH_{7.5}$ and C_2ASH_8 in the PRT. These changes to the reaction products result in the measured Q and CH consumed to drop from 803 to 714 J/g_{SCM} and 157 to 110 g/100 g_{SCM}, respectively. Note that the formation of different types of carboaluminate phases depends on the CO_2-SO_3-Al_2O_3 balance,[72] and this balance needs to be considered in the interpretation of the Q and CH consumed in the PRT. The Q and CH consumed by the carbonate reactions with Al_2O_3 in the PRT is summarized in Table 1. As the SiO_2 is increased from 33 to 90%, C-S-H phases form in addition to C_2ASH_8 and carboaluminate phases, which results in an increased Q and CH consumed. Above a 90% SiO_2 content, all the alumina is bound as carboaluminates and there is no alumina available to react with the SiO_2 and CH to form C_2ASH_8, and only carboaluminates and C-S-H phases form. When the SCM is 100% SiO_2, only C-S-H phases form. It can be noted that the addition of 20 g gypsum (Fig. 6(a)) and 5 g $CaCO_3$ (Fig. 7(a)) show a similar trend in the phases that form. This is because the resulting phases are both AFm phases (monosulfate forms when gypsum is added, and hemicarbonates/monocarbonates form when $CaCO_3$ is added, which both fall under the AFm family of phases).

If carbonates are added during the measurement of reactivity, as it is done in the R3 test, the reactions that form carboaluminate need to be accounted for while determining the reactivity of the SCM using the Q and the CH consumed.[33] This can be done by accounting for the mass of alumina from the SCM that reacts with the carbonates. Figure 7(b) shows an example of the modification to the reactivity lines made for varying SiO_2 to Al_2O_3 ratios in an SCM when 5 g $CaCO_3$ is added. As expected, the 100% SiO_2 line is unaffected by the presence of carbonates. As the alumina content of the SCM increases, the top of the lines (100% DOR* point in each line) moves in the same manner as explained in the previous paragraph and shown in Fig. 7(b) using the arrow. Similar to the lines when sulfates are added, it can be noted that some lines have kinks/bends on them due to the preferential reaction of alumina with carbonates to form carboaluminate. The location of the kink on a line of given composition is the point at which the reactive alumina exceeds the amount of alumina that can be consumed in the reaction that produces carboaluminates—that is, for DOR* values below the kink in the line, only carboaluminates form, for the DOR* values above the kink in the line, carboaluminates and $C_2AH_{7.5}$ + C_2ASH_8 form. As such, most commercial SCMs contain high levels of silica and low levels of alumina, which can pose a challenge while measuring the reactivity using the PRT when carbonates are present due to the varying amounts and composition of the carboaluminates that can form. Therefore, the addition of sulfates and carbonates is not recommended while measuring the reactivity of SCMs.

RECOMMENDATIONS ON CALCULATING REACTIVITY OF COMMERCIAL SCMs

This study shows that the interpretation of the reactivity test outputs to quantify reactivity can be challenging. For example, the PRT uses two theoretical reactivity lines (100% Al_2O_3 line and the 100% SiO_2 line) to interpolate and quantify the reactivity of the SCM.[23,33] It is shown in this paper that interpretation of the reactivity test outputs might need to be to be customized based on the type of SCM and its composition. It is recommended to interpret the reactivity of different classes of SCMs based on their chemical composition, using similar classifications made by standard SCM specifications and experimental data from the literature.[23,33,46,49-51,55,58-60] For PRT, in this paper, these compositional classifications are used to determine the most appropriate ways to interpret the reactivity test results for typical commercial SCMs (silica fume [SF], fly ash [FA] and natural pozzolans [NP], calcined clays [CC], and slags) for a more accurate calculation of DOR* in the PRT. Any commercial SCM tested in the PRT would fall between the bounding reactivity lines for that SCM type, shown in Table 2. The deviation in the calculated value of DOR* from the actual value of DOR* for any composition within the bounding compositions is also calculated to assess the accuracy of using these bounding lines.

The DOR* can also be quantified in the PRT using Eq. (1). In the equation, a_1 and a_2 are constants that depend on the test parameters and the chemical composition of the reactivity lines used. The values of a_1 and a_2 (shown in Table 2), therefore, will vary for each SCM, as different lines will be used for each SCM. Note that the values of a_1 and a_2 are computed from the predicted Q and CH consumed obtained in the simulations for each class of SCM.

Silica fume

Silica fume is specified to contain a minimum of 85% SiO_2 as per ASTM C1240.[71] The remaining constituents can be loss on ignition (LOI), Al_2O_3, CaO, or other impurities. Typical commercially available silica fumes contain >90% SiO_2 and have CaO or LOI as the impurity.[33,46,49,50,55] Therefore, the proposed reactivity lines to use are the 100% SiO_2 line and 85% SiO_2 + 15% CaO line. The experimental

Table 2—Typical chemical composition of commercial SCMs in this study

SCM	Left line	Right line	a_1, 1/(J/g_{SCM}))	a_2, 1/(g/100 g_{SCM}))
SF	85% SiO_2 + 15% CaO	100% SiO_2	1.00×10^{-3}	1.15×10^{-3}
FA and NP	82% SiO_2 + 18% CaO	100% SiO_2	1.00×10^{-3}	1.16×10^{-3}
CC	50% SiO_2 + 50% Al_2O_3	75% SiO_2 + 25% Al_2O_3	1.81×10^{-3}	-1.95×10^{-3}
Slags	18% SiO_2 + 50% CaO + 32% Al_2O_3	70% SiO_2 + 30% CaO	1.12×10^{-3}	1.13×10^{-4}

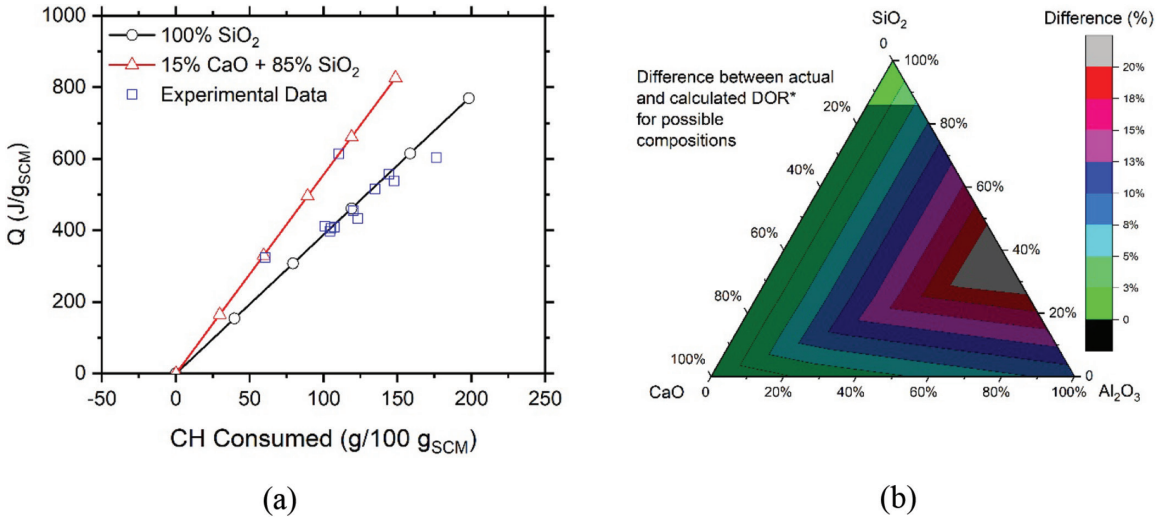

Fig. 8—(a) Reactivity lines and experimental results for silica fume; and (b) difference between actual and calculated when using reactivity lines for calculation of reactivity. Highlighted zone represents commercial silica fume compositions.

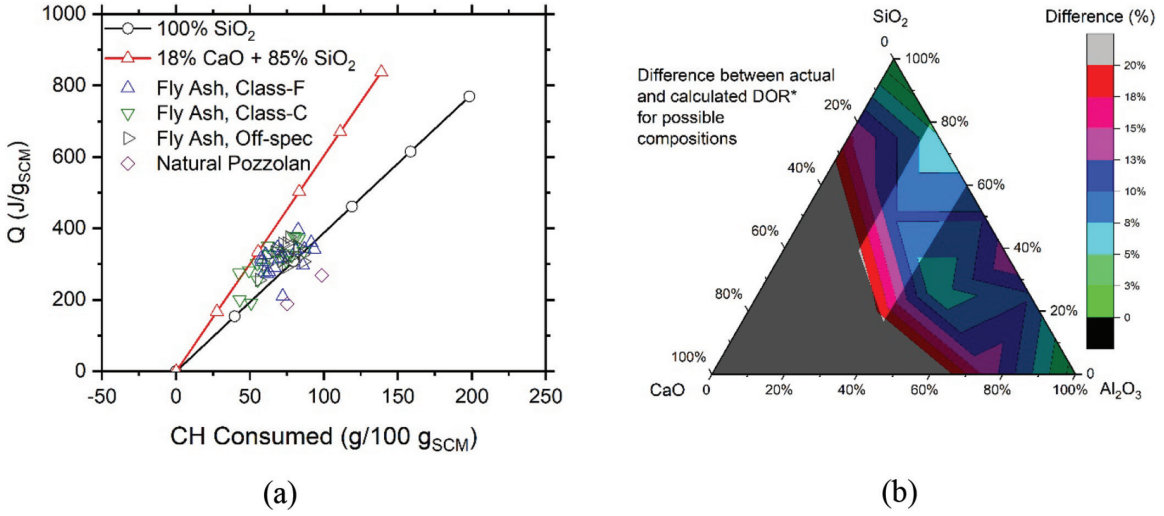

Fig. 9—(a) Reactivity lines and experimental results for fly ash; and (b) difference between actual and calculated DOR when using reactivity lines for calculation of reactivity.*

results from literature[33,46,49,50,55] are plotted, along with the recommended reactivity lines, as shown in Fig. 8(a). All the data points fall within 20 g CH consumed per 100 g_{SCM} or 50 J/g_{SCM} of the reactivity lines. Figure 8(b) shows the difference between the calculated DOR* from the actual DOR* when Eq. (2) and the constants in Table 2 are used. It should be noted from this plot that the difference in the calculated reactivity and actual reactivity for any composition is under 5%, and therefore, these lines provide an accurate measure of DOR* and should be used for the calculation of DOR* of silica fumes.

Fly ash and natural pozzolans

ASTM C618[25] specifies the chemical compositional requirements for Class F and Class C fly ashes as well as natural pozzolans. Fly ashes conforming to ASTM C618 are to contain >50% by mass of $SiO_2 + Al_2O_3 + Fe_2O_3$. Class F fly ashes are to contain less than 18% CaO and Class C fly ashes can contain more than 18% CaO. However, from the experimental data available in the literature,[33,46,49,50,55] the lines chosen for both classes of fly ash, as well as natural pozzolans, are the 100% SiO_2 line and 82% SiO_2 + 18% CaO line, as they represent the bounding cases for the experimental data. The experimental results from literature[33,46,49,50,55] are plotted along with the recommended reactivity lines, as shown in Fig. 9(a). All the data points fall within 20 g CH consumed per 100 g_{SCM} or 50 J/g_{SCM} of the reactivity lines. Figure 9(b) shows the difference in the calculated DOR* from the actual DOR* when Eq. (2) and the constants in Table 2 are used for any chemical composition of fly ash that satisfies the ASTM C618[25] requirements, which can be obtained commercially. The difference in the calculated DOR* from the actual DOR* for typical commercially available ash and natural pozzolan compositions is under 13% for CaO < 40% when the actual DOR* is 100%. It should be noted that if the DOR* is lower, the associated difference between the actual and calculated DOR* will also be proportionally lower. Because the typical DOR* of fly ashes is approximately 40%, this difference between the actual and predicted DOR* would be only approximately 5%.

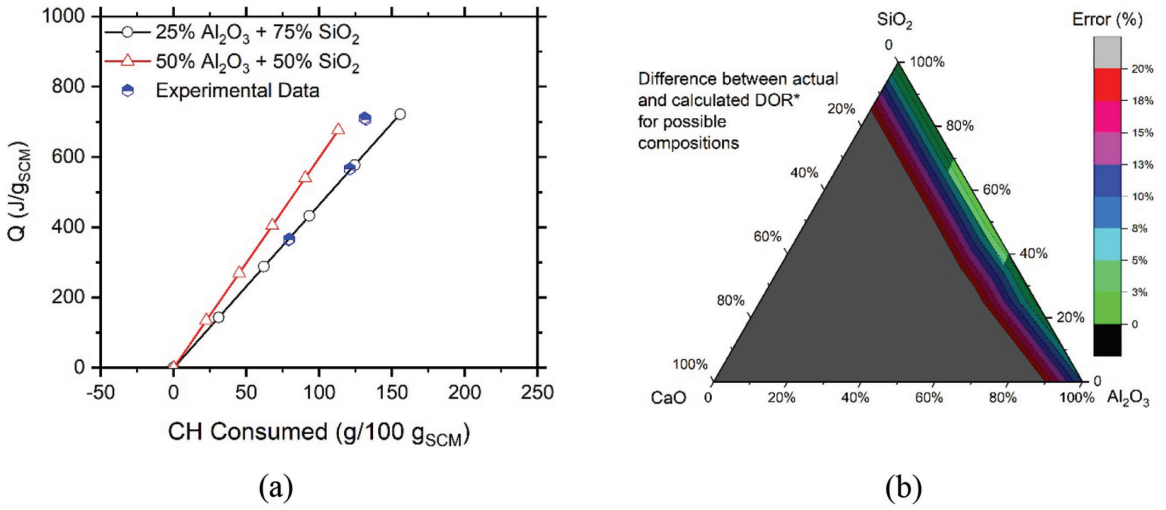

Fig. 10—(a) Reactivity lines and experimental results for calcined clays and metakaolin; and (b) difference between actual and calculated DOR when using reactivity lines for calculation of reactivity.*

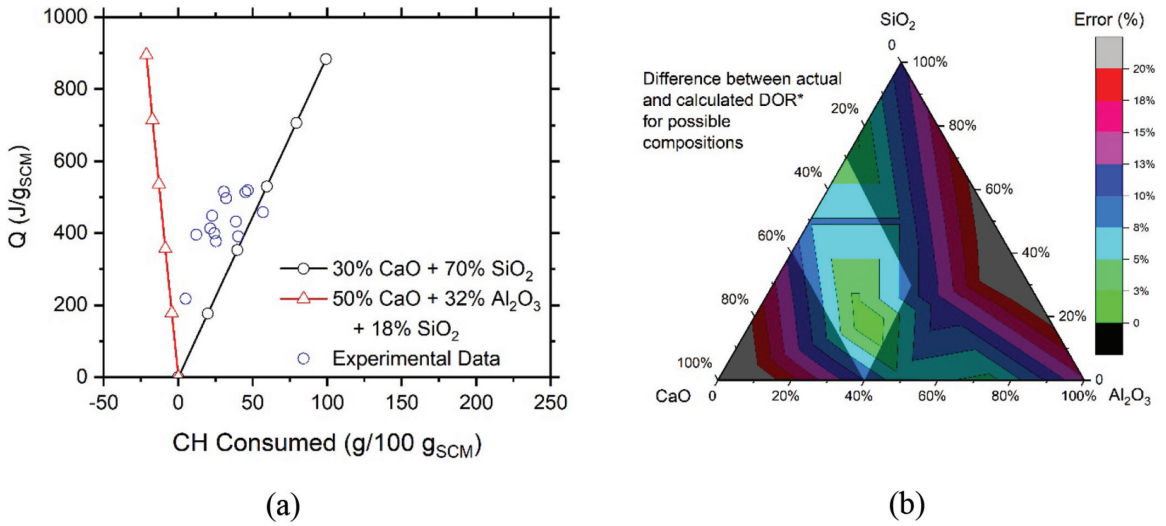

Fig. 11—(a) Reactivity lines and experimental results for slag; and (b) difference between actual and calculated DOR when using reactivity lines for calculation of reactivity.*

Calcined clays and metakaolin

Calcined clays and metakaolin typically contain high amounts of alumina (20 to 50%[55]), and high amounts of silica with negligible CaO, with the typical chemical composition obtained from the literature shown in Table 2. The lines chosen for calcined clays and metakaolin are the 75% SiO_2 +25% Al_2O_3 line and 50% SiO_2 + 50% Al_2O_3 line. The experimental results from literature[33,46,49,50,55] are plotted along with the recommended reactivity lines as shown in Fig. 10(a). All the data points fall within the bounding reactivity lines. Figure 10(b) shows the difference in the calculated DOR* from the actual DOR* when Eq. (2) and the constants in Table 2 are used for any chemical composition of fly ash that satisfies the ASTM C618[25] requirements, which can be obtained commercially. This difference between the calculated and actual reactivity for typical commercially available calcined clays and metakaolin compositions is under 5%. Therefore, for calcined clays and metakaolin, using the 75% SiO_2 + 25% Al_2O_3 line and the 50% SiO_2 + 50% Al_2O_3 line to calculate the DOR* is recommended.

Slag

ASTM C989/C989M[73] specifies the chemical compositional requirements for the use of slag (slag cements); however, the only limitation on the chemistry specified is a maximum sulfide content of 2%. Therefore, the commercially available slag compositions from the literature[33,46,49,50,55] is used to obtain the optimal reactivity lines. Typical slags available in the United States[33,46,49,50,55] contain 20 to 40% SiO_2, 10 to 15% Al_2O_3, and 30 to 50% CaO. Therefore, the reactivity lines chosen to best represent the data and calculate the reactivity is the 70% SiO_2 + 30% CaO line and 18% SiO_2 + 32% Al_2O_3 + 50% CaO line. The experimental results from the literature[33,46,49,50,55] are plotted along with the recommended reactivity lines as shown in Fig. 11(a). All but one data point fall within the bounding reactivity lines. Figure 11(b) shows the difference in the calculated DOR* from the actual DOR* when Eq. (2) and the constants in Table 2 are used for any typical slag available commercially. The difference between the calculated reactivity and actual DOR* for typical commercially available slag is under 13%

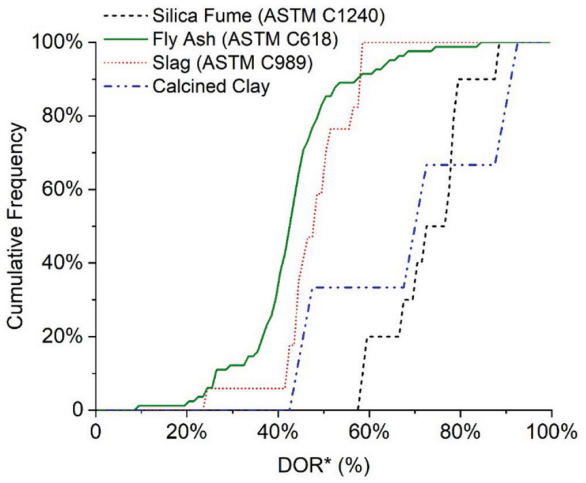

Fig. 12—Cumulative frequency plot of reactivities for commercial SCMs.

when these lines are used and, as such, the use of the 70% SiO_2 + 30% CaO line and 18% SiO_2 + 32% Al_2O_3 + 50% CaO line is recommended.

A cumulative frequency plot of the reactivities determined using experimental data in the literature[23,33,46,49,50,55,59,60] is shown in Fig. 12. This statistical distribution enables a comparison of SCMs based on their DOR* (which is a performance indicator of the SCM[39]). For example, a fly ash of 60% reactivity can be considered a highly reactive fly ash but a silica fume of 60% reactivity may be considered a low-reactivity silica fume. The range of silica fume reactivity can be seen to be from 54 to 90% (mean reactivity is 71%) while fly ash ranges from 9 to 85% (mean reactivity is 43%).

CONCLUSIONS

This paper uses thermodynamic modeling to aid the interpretation of pozzolanic reactivity testing of different classes of supplementary cementitious materials (SCMs). The following conclusions were drawn:

1. The investigation of the SCMs containing only SiO_2 and Al_2O_3 (no CaO) showed that as the ratio of SiO_2 to Al_2O_3 varies, the phase assemblage changes (pure Al_2O_3 results in the formation of $C_2AH_{7.5}$, pure SiO_2 results in the formation of C-S-H phases, and combinations of SiO_2 and Al_2O_3 result in the formation of C_2ASH_8 along with C-S-H or $C_2AH_{7.5}$). The heat release (Q) and calcium hydroxide (CH) consumed follow a response that is roughly bilinear, with the minima of heat release and CH consumed being at SiO_2:Al_2O_3 where only C_2ASH_8 forms.

2. The investigation of the SCMs containing SiO_2, Al_2O_3, and CaO showed that the presence of CaO in an SCM results in a net reduction in the measured CH consumed as the CaO in the SCM provides an internal source of Ca. The Q increases as the reaction of CaO is more exothermic than the reactions of SiO_2 and Al_2O_3.

3. The study of the influence of the presence of sulfates and carbonates during reactivity quantification indicated that both sulfates and carbonates alter the reaction of the Al_2O_3 phases. The Al_2O_3 reacts preferentially with sulfates and carbonates to form AFm phases (Al_2O_3 reacts with sulfates to form monosulfate, and with carbonates to form carboaluminates). The reaction forming these AFm phases is more exothermic than the reaction that forms $C_2AH_{7.5}$ or C_2ASH_8. As such, the addition of sulfates and carbonates in the quantification of the pozzolanic reactivity is not recommended, as it makes the interpretation of the results challenging as the reactions are altered with reactions other than pozzolanic reactions occurring.

4. Following Conclusions 1 through 3, it was shown that the reactivity of commercial SCMs should be interpreted specific to the type of SCM as described by ASTM International/AASHTO. The proposed interpretation is provided in this paper. This implies that directly comparing the Q is only applicable with SCMs of the same type.

5. The statistical data on the reactivities of commercially available SCMs using the proposed approach indicate that the mean reactivity of silica fume is 70%, the mean reactivity of fly ash + natural pozzolan is 43%, and the mean reactivity of slags is 48%.

Overall, this paper provides a fundamental understanding of the reactions that occur in the pozzolanic reactivity test (PRT), demonstrates the robustness of the PRT, extends the scope of the PRT to measure the reactivity of pozzolanic as well as hydraulic SCMs, and is intended to aid in the interpretation of the results of the PRT and allow for a more accurate determination of the degree of reactivity (DOR*).

AUTHOR BIOS

ACI member **Keshav Bharadwaj** *is a Postdoctoral Scholar at Oregon State University, Corvallis, OR, where he received his PhD in civil engineering. His research interests include thermodynamic modeling, reactivity, transport in cementitious systems, and linking the microstructure of concrete to the engineering performance of concrete.*

O. Burkan Isgor, *FACI, is a Professor in the School of Civil and Construction Engineering at Oregon State University. He is Chair of ACI Committee 222, Corrosion of Metals in Concrete, and a member of ACI Committees 236, Material Science of Concrete, and 365, Service Life Prediction. His research interests include corrosion of steel in concrete, service-life modeling, and thermodynamic modeling of cementitious systems.*

W. Jason Weiss, *FACI, is the Edwards Distinguished Professor of Engineering in the School of Civil and Construction Engineering at Oregon State University. He is Editor-in-Chief of the* ACI Materials Journal *and a member of the ACI Technical Activities Committee.*

ACKNOWLEDGMENTS

The authors gratefully acknowledge the financial support provided by ARPA-E (Advanced Research Projects Agency-Energy), EPRI (Electric Power Research Institute), CALTRANS (California Department of Transportation), and National Science Foundation (Grant No. NSF CMMI 1728358). The authors gratefully acknowledge support from the John and Jean Loosely Chair and the Edwards Distinguished Chair at Oregon State, who have supported the last two authors, respectively.

REFERENCES

1. Thomas, M., *Supplementary Cementing Materials in Concrete*, CRC Press, Boca Raton, FL, 2013, 210 pp.

2. Bredy, P.; Chabannet, M.; and Pera, J., "Microstructure and Porosity of Metakaolin Blended Cements," MRS Online Proceedings Library Archive, V. 137, 1988.

3. Bharadwaj, K.; Ghantous, R. M.; Sahan, F. N.; Isgor, B. O.; and Weiss, J., "Predicting Pore Volume, Compressive Strength, Pore Connectivity, and Formation Factor in Cementitious Pastes Containing Fly Ash," *Cement and Concrete Composites*, V. 122, Paper No. 104113, 2021.

4. Lothenbach, B.; Scrivener, K.; and Hooton, R. D., "Supplementary Cementitious Materials," *Cement and Concrete Research*, V. 41, No. 12, 2011, pp. 1244-1256. doi: 10.1016/j.cemconres.2010.12.001

5. Poon, C.-S.; Kou, S.; and Lam, L., "Compressive Strength, Chloride Diffusivity and Pore Structure of High Performance Metakaolin and Silica Fume Concrete," *Construction and Building Materials*, V. 20, No. 10, 2006, pp. 858-865. doi: 10.1016/j.conbuildmat.2005.07.001

6. Pepper, L., and Mather, B., "Effectiveness of Mineral Admixtures in Preventing Excessive Expansion of Concrete Due to Alkali-Aggregate Reaction," *American Society for Testing Materials - Proceedings*, Philadelphia, PA, 1959.

7. Thomas, M., "The Effect of Supplementary Cementing Materials on Alkali-Silica Reaction: A Review," *Cement and Concrete Research*, V. 41, No. 12, 2011, pp. 1224-1231. doi: 10.1016/j.cemconres.2010.11.003

8. Suraneni, P.; Azad, V. J.; Isgor, B. O.; and Weiss, W. J., "Calcium Oxychloride Formation in Pastes Containing Supplementary Cementitious Materials: Thoughts on the Role of Cement and Supplementary Cementitious Materials Reactivity," *RILEM Technical Letters*, V. 1, 2016, pp. 24-30. doi: 10.21809/rilemtechlett.2016.7

9. Suraneni, P.; Azad, V. J.; Isgor, O. B.; and Weiss, W. J., "Deicing Salts and Durability of Concrete Pavements and Joints," *Concrete International*, V. 38, No. 4, Apr. 2016, pp. 48-54.

10. Suraneni, P.; Azad, V. J.; Isgor, O. B.; and Weiss, W. J., "Use of Fly Ash to Minimize Deicing Salt Damage in Concrete Pavements," *Transportation Research Record: Journal of the Transportation Research Board*, V. 2629, No. 1, 2017, pp. 24-32. doi: 10.3141/2629-05

11. Whatley, S. N.; Suraneni, P.; Azad, V. J.; Isgor, O. B.; and Weiss, J., "Mitigation of Calcium Oxychloride Formation in Cement Pastes Using Undensified Silica Fume," *Journal of Materials in Civil Engineering*, ASCE, V. 29, No. 10, Paper No.04017198, 2017. doi: 10.1061/(ASCE)MT.1943-5533.00020

12. Juenger, M. C.; Snellings, R.; and Bernal, S. A., "Supplementary Cementitious Materials: New Sources, Characterization, and Performance Insights," *Cement and Concrete Research*, V. 122, 2019, pp. 257-273. doi: 10.1016/j.cemconres.2019.05.008

13. Butalia, T. S., "Beneficial Use of Ponded Fly Ash in Structural Concrete," UKIERI Concrete Congress Key Note Address, Jalandhar: Dr. B. R. Ambedkar National Institute of Technology, Jalandhar, Punjab, India, 2019.

14. Innocenti, G.; Benkeser, D. J.; Dase, J. E.; Wirth, X.; Sievers, C.; and Kurtis, K. E., "Beneficiation of Ponded Coal Ash through Chemi-Mechanical Grinding," *Fuel*, V. 299, Paper No.120892, 2021.

15. Clavier, K. A.; Paris, J. M.; Ferraro, C. C.; and Townsend, T. G., "Opportunities and Challenges Associated with Using Municipal Waste Incineration Ash as a Raw Ingredient in Cement Production—A Review," *Resources, Conservation and Recycling*, V. 160, Paper No.104888, 2020.

16. Bahurudeen, A.; Kanraj, D.; Gokul Dev, V.; and Santhanam, M., "Performance Evaluation of Sugarcane Bagasse Ash Blended Cement in Concrete," *Cement and Concrete Composites*, V. 59, 2015, pp. 77-88. doi: 10.1016/j.cemconcomp.2015.03.004

17. Bahurudeen, A.; Marckson, A.; Kishore, A.; and Santhanam, M., "Development of Sugarcane Bagasse Ash Based Portland Pozzolana Cement and Evaluation of Compatibility with Superplasticizers," *Construction and Building Materials*, V. 68, 2014, pp. 465-475. doi: 10.1016/j.conbuildmat.2014.07.013

18. Bahurudeen, A., and Santhanam, M., "Influence of Different Processing Methods on the Pozzolanic Performance of Sugarcane Bagasse Ash," *Cement and Concrete Composites*, V. 56, 2015, pp. 32-45. doi: 10.1016/j.cemconcomp.2014.11.002

19. PCA, *Design and Control of Concrete Mixtures*, Portland Cement Association, Skokie, IL, 2012, 459 pp.

20. Bharadwaj, K.; Isgor, B. O.; Weiss, J. W.; Chopperla, K. S. T.; Choudhary, A.; Vasudevan, G.; Glosser, D.; Ideker, J.; and Trejo, D., "A New Mixture Proportioning Method for Performance-Based Concrete," *ACI Materials Journal*, V. 119, No. 2, Mar. 2022, pp. 207-220.

21. Mehta, P. K., and Monteiro, P. J., *Concrete: Microstructure, Properties and Materials*, McGraw Hill Professional, New Delhi, India, 2006, 675 pp.

22. Taylor, H. F., *Cement Chemistry*, Thomas Telford, London, UK, 1997, 459 pp.

23. Glosser, D.; Choudhary, A.; Isgor, O. B.; and Weiss, W. J., "Investigation of Reactivity of Fly Ash and Its Effect on Mixture Properties," *ACI Materials Journal*, V. 116, No. 4, July 2019, pp. 193-200. doi: 10.14359/51716722

24. Glosser, D.; Suraneni, P.; Isgor, O. B.; and Weiss, W. J., "Estimating Reaction Kinetics of Cementitious Pastes Containing Fly Ash," *Cement and Concrete Composites*, V. 112, Paper No. 103655, 2020.

25. ASTM C618-19, "Standard Specification for Coal Fly Ash and Raw or Calcined Natural Pozzolan for Use in Concrete," ASTM International, West Conshohocken, PA, 2019.

26. AASHTO M 295, "Standard Specification for Coal Fly Ash and Raw or Calcined Natural Pozzolan for Use in Concrete," American Association of State Highway and Transportation Officials (AASHTO), Washington, DC, 2019.

27. EN 206-1, "Concrete—Part 1: Specification, Performance, Production and Conformity," European Committee for Standardization, Brussels, Belgium, 2000.

28. Papadakis, V. G., and Tsimas, S., "Supplementary Cementing Materials in Concrete: Part I: Efficiencya Design," *Cement and Concrete Research*, V. 32, No. 10, 2002, pp. 1525-1532. doi: 10.1016/S0008-8846(02)00827-X

29. Glosser, D.; Suraneni, P.; Isgor, O. B.; and Weiss, W. J., "Using Glass Content to Determine the Reactivity of Fly Ash for Thermodynamic Calculations," *Cement and Concrete Composites*, V. 115, Paper No.103849, 2021.

30. Durdziński, P. T.; Dunant, C. F.; Haha, M. B.; and Scrivener, K. L., "A New Quantification Method Based on Sem-Eds to Assess Fly Ash Composition and Study the Reaction of Its Individual Components in Hydrating Cement Paste," *Cement and Concrete Research*, V. 73, 2015, pp. 111-122. doi: 10.1016/j.cemconres.2015.02.008

31. EN 196-5, "Methods of Testing Cement—Part 5: Pozzolanicity Test for Pozzolanic Cement," European Committee for Standardization, Brussels, Belgium, 2011.

32. Chapelle, J., "Attaque sulfo-calcique des laitiers et des pouzzolanes," *Imprimerie Centrale de l'Ortois-Orras*, 1958, pp. 193-201.

33. Choudhary, A.; Bharadwaj, K.; Ghantous, R. M.; Isgor, B.; and Weiss, J., "Pozzolanic Reactivity Test of Supplementary Cementitious Materials," *ACI Materials Journal*, V. 119, No. 2, Mar. 2022, pp. 255-268.

34. Thorstensen, R. T., and Fidjestol, P., "Inconsistencies in the Pozzolanic Strength Activity Index (SAI) for Silica Fume According To EN and ASTM," *Materials and Structures*, V. 48, No. 12, 2015, pp. 3979-3990. doi: 10.1617/s11527-014-0457-6

35. Bentz, D. P.; Durán-Herrera, A.; and Galvez-Moreno, D., "Comparison of ASTM C311 Strength Activity Index Testing Versus Testing Based on Constant Volumetric Proportions," *Journal of ASTM International*, V. 9, No. 1, 2011, pp. 1-7.

36. ASTM C1897-20, "Standard Test Method for Measuring the Reactivity of Supplementary Cementitious Materials by Isothermal Calorimetry and Bound Water Measurements," ASTM International, West Conshohocken, PA, 2020.

37. Avet, F.; Snellings, R.; Alujas Diaz, A.; Ben Haha, M.; and Scrivener, K., "Development of a New Rapid, Relevant and Reliable (R-3) Test Method to Evaluate the Pozzolanic Reactivity of Calcined Kaolinitic Clays," *Cement and Concrete Research*, V. 85, 2016, pp. 1-11. doi: 10.1016/j.cemconres.2016.02.015

38. Snellings, R., and Scrivener, K. L., "Rapid Screening Tests for Supplementary Cementitious Materials: Past and Future," *Materials and Structures*, V. 49, No. 8, 2016, pp. 3265-3279. doi: 10.1617/s11527-015-0718-z

39. Bharadwaj, K.; Isgor, B. O.; and Weiss, J. W., "A Simplified Approach to Determine the Pozzolanic Reactivity of Commercial Supplementary Cementitious Materials," *Concrete International*, V. 44, No. 1, Jan. 2022, pp. 27-32.

40. Azad, V. J.; Suraneni, P.; Trejo, D.; Weiss, W. J.; and Isgor, O. B., "Thermodynamic Investigation of Allowable Admixed Chloride Limits in Concrete," *ACI Materials Journal*, V. 115, No. 5, Sept. 2018, pp. 727-738. doi: 10.14359/51702349

41. Bharadwaj, K.; Chopperla, K. S. T.; Choudhary, A.; Glosser, D.; Ghantous, R. M.; Vasudevan, G.; Ideker, J. H.; Isgor, B.; Trejo, D.; and Weiss, J. W., "Caltrans: Impact of the Use of Portland-Limestone Cement on Concrete Performance as Plain or Reinforced Material—Final Report," Oregon State University, Corvallis, OR, 320 pp.

42. Bharadwaj, K.; Glosser, D.; Moradllo, M. K.; Isgor, O. B.; and Weiss, J., "Toward the Prediction of Pore Volumes and Freeze-Thaw Performance of Concrete Using Thermodynamic Modelling," *Cement and Concrete Research*, V. 124, Paper No. 105820, 2019.

43. Bharadwaj, K.; Isgor, B. O.; and Weiss, J. W., "Supplementary Cementitious Materials in Portland Limestone Cements," *ACI Materials Journal*, V. 119, No. 2, Mar. 2022, pp. 141-154.

44. Choudhary, A.; Ghantous, R. M.; Bharadwaj, K.; Opdahl, O. H.; Isgor, B. O.; and Weiss, J. W., "Electrical and Transport Properties of Cement Mortar Made Using Portland Limestone Cement," *Advances in Civil Engineering Materials*, V. 11, No. 1, 2022, pp. 263-279. doi: 10.1520/ACEM20210119

45. Glosser, D.; Azad, V. J.; Suraneni, P.; Isgor, B.; and Weiss, J., "Extension of Powers-Brownyard Model to Pastes Containing Supplementary Cementitious Materials," *ACI Materials Journal*, V. 116, No. 5, Sept. 2019, pp. 205-216. doi: 10.14359/51714466

46. Suraneni, P., and Weiss, J., "Examining the Pozzolanicity of Supplementary Cementitious Materials Using Isothermal Calorimetry and Thermogravimetric Analysis," *Cement and Concrete Composites*, V. 83, 2017, pp. 273-278. doi: 10.1016/j.cemconcomp.2017.07.009

47. Glosser, D.; Isgor, O. B.; and Weiss, W. J., "Non-Equilibrium Thermodynamic Modeling Framework for Ordinary Portland Cement/

Supplementary Cementitious Material Systems," *ACI Materials Journal*, V. 117, No. 6, Nov. 2020, pp. 111-123.

48. Ramanathan, S., "Reactivity of Supplementary Cementitious Materials in Model Systems and Cementitious Pastes," PhD thesis, University of Miami, Miami, FL, 2021.

49. Ramanathan, S.; Croly, M.; and Suraneni, P., "Comparison of the Effects that Supplementary Cementitious Materials Replacement Levels Have on Cementitious Paste Properties," *Cement and Concrete Composites*, V. 112, Paper No. 103678, 2020.

50. Ramanathan, S.; Kasaniya, M.; Tuen, M.; Thomas, M. D.; and Suraneni, P., "Linking Reactivity Test Outputs to Properties of Cementitious Pastes Made with Supplementary Cementitious Materials," *Cement and Concrete Composites*, V. 114, Paper No. 103742, 2020.

51. Ramanathan, S.; Moon, H.; Croly, M.; Chung, C.-W.; and Suraneni, P., "Predicting the Degree of Reaction of Supplementary Cementitious Materials in Cementitious Pastes Using a Pozzolanic Test," *Construction and Building Materials*, V. 204, 2019, pp. 621-630. doi: 10.1016/j.conbuildmat.2019.01.173

52. Ramanathan, S.; Perumal, P.; Illikainen, M.; and Suraneni, P., "Mechanically Activated Mine Tailings for Use as Supplementary Cementitious Materials," *RILEM Technical Letters*, V. 6, 2021, pp. 61-69. doi: 10.21809/rilemtechlett.2021.143

53. Ramanathan, S.; Pestana, L. R.; and Suraneni, P., "Reaction Kinetics of Supplementary Cementitious Materials in Reactivity Tests," *Cement*, Paper No. 100022, 2022.

54. Ramanathan, S.; Suraneni, P.; Wang, Y.; Shan, H.; Hajibabaee, A.; and Weiss, J., "Combining Reactivity Test, Isothermal Calorimetry, and Compressive Strength Measurements to Study Conventional and Alternative Supplementary Cementitious Materials," *Proceedings of the International Conference of Sustainable Production and Use of Cement and Concrete*, 2020, pp. 445-454.

55. Suraneni, P.; Hajibabaee, A.; Ramanathan, S.; Wang, Y.; and Weiss, J., "New Insights from Reactivity Testing of Supplementary Cementitious Materials," *Cement and Concrete Composites*, V. 103, 2019, pp. 331-338. doi: 10.1016/j.cemconcomp.2019.05.017

56. Suraneni, P., and Ramanathan, S., "Reactivity of Tested SCMs," personal communication sent to W. J. Weiss, K. Bharadwaj, and B. O. Isgor, 2020.

57. Ramanathan, S.; Tuen, M.; and Suraneni, P., "Influence of Supplementary Cementitious Material and Filler Fineness on Their Reactivity in Model Systems and Cementitious Pastes," *Materials and Structures*, V. 55, No. 5, 2022, 25 pp. doi: 10.1617/s11527-022-01980-2

58. Moradllo, M. K.; Chung, C.-W.; Keys, M. H.; Choudhary, A.; Reese, S. R.; and Weiss, W. J., "Use of Borosilicate Glass Powder in Cementitious Materials: Pozzolanic Reactivity and Neutron Shielding Properties," *Cement and Concrete Composites*, V. 112, Paper No. 103640, 2020.

59. Burroughs, J. F., "Influence of Chemical and Physical Properties of Poorly-Ordered Silica on Reactivity and Rheology of Cementitious Materials," PhD thesis, Purdue University, West Lafayette, IN, 2019.

60. Isgor, B.; Ideker, J.; Trejo, D.; Weiss, J.; Bharadwaj, K.; Choudhary, A.; Teja, C. K. S.; Glosser, D.; and Vasudevan, G., "Development of a Performance-Based Mixture Proportioning Procedure for Concrete Incorporating Off-Spec Fly Ash," Energy Power Research Institute (EPRI), Palo Alto, CA, 78 pp.

61. Kim, T., and Olek, J., "Effects of Sample Preparation and Interpretation of Thermogravimetric Curves on Calcium Hydroxide in Hydrated Pastes and Mortars," *Transportation Research Record: Journal of the Transportation Research Board*, V. 2290, No. 1, 2012, pp. 10-18. doi: 10.3141/2290-02

62. Lothenbach, B.; Matschei, T.; Möschner, G.; and Glasser, F. P., "Thermodynamic Modelling of the Effect of Temperature on the Hydration and Porosity of Portland Cement," *Cement and Concrete Research*, V. 38, No. 1, 2008, pp. 1-18. doi: 10.1016/j.cemconres.2007.08.017

63. Lothenbach, B., and Winnefeld, F., "Thermodynamic Modelling of the Hydration of Portland Cement," *Cement and Concrete Research*, V. 36, No. 2, 2006, pp. 209-226. doi: 10.1016/j.cemconres.2005.03.001

64. Kulik, D. A.; Wagner, T.; Dmytrieva, S. V.; Kosakowski, G.; Hingerl, F. F.; Chudnenko, K. V.; and Berner, U. R., "Gem-Selektor Geochemical Modeling Package: Revised Algorithm and GEMS3K Numerical Kernel for Coupled Simulation Codes," *Computational Geosciences*, V. 17, No. 1, 2013, pp. 1-24.

65. Lothenbach, B.; Kulik, D. A.; Matschei, T.; Balonis, M.; Baquerizo, L.; Dilnesa, B.; Miron, G. D.; and Myers, R. J., "Cemdata 18: A Chemical Thermodynamic Database for Hydrated Portland Cements and Alkali-Activated Materials," *Cement and Concrete Research*, V. 115, 2019, pp. 472-506. doi: 10.1016/j.cemconres.2018.04.018

66. Gosselin, C., "Microstructural Development of Calcium Aluminate Cement Based Systems with and without Supplementary Cementitious Materials," PhD thesis, Swiss Federal Institute of Technology Lausanne, Lausanne, Switzerland, 234 pp.

67. Choudhary, A., "The Pozzolanic Reactivity Test and the Properties of Portland Limestone Cement," PhD thesis, Oregon State University, Corvallis, OR, 2021.

68. NIST, "NIST Chemistry WebBook," National Institute of Standards and Technology (NIST), Gaithersburg, MD, 2021, doi: 10.18434/T4D30310.18434/T4D303

69. de Silva, P., and Glasser, F. P., "Phase Relations in the System CaO Al_2O_3 SiO_2 H_2O Relevant to Metakaolin-Calcium Hydroxide Hydration," *Cement and Concrete Research*, V. 23, No. 3, 1993, pp. 627-639. doi: 10.1016/0008-8846(93)90014-Z

70. AASHTO M 307, "Standard Specification for Silica Fume Used in Cementitious Mixtures," American Association of State Highway and Transportation Officials, Washington, DC, 2013.

71. ASTM C1240-20, "Standard Specification for Silica Fume Used in Cementitious Mixtures," ASTM International, West Conshohocken, PA, 2020.

72. Matschei, T.; Lothenbach, B.; and Glasser, F., "The AFM Phase in Portland Cement," *Cement and Concrete Research*, V. 37, No. 2, 2007, pp. 118-130. doi: 10.1016/j.cemconres.2006.10.010

73. ASTM C989/C989M-18a, "Standard Specification for Slag Cement for Use in Concrete and Mortars," ASTM International, West Conshohocken, PA, 2018.

APPENDIX A – INFLUENCE OF C-S-H MODEL USED ON PREDICTIONS

CemData v18.01 (65) contains several C-S-H models available to predict the various forms of C-S-H that typically form. Typically for siliceous systems, the CSHQ model (74) is used, and to model high Al systems when portlandite is depleted, or to model alkali activated systems the CNASH model (75, 76) is used. In the main body of this paper, the CSHQ model was used to model the reaction of SiO_2+Al_2O_3 SCMs in the PRT, shown in Figure 2.

Figure A-1 (a) shows the predicted phase assemblage, Q, and CH consumed predicted by the CNASH model when an SCM that is a combination of SiO_2+Al_2O_3 is tested in the PRT. The model predicts that 100% Al_2O_3 reacts to form $C_2AH_{7.5}$ as is the case when the CSHQ model is used. As the SiO_2 in the SCM is increased from 0% to 33%, C_2ASH_8 forms in addition to $C_2AH_{7.5}$. This is accompanied with a decrease in Q and CH consumed. At a 33% SiO_2+67%Al_2O_3, the SCM is predicted to form only C_2ASH_8, and this reaction consumes the least CH. As the SiO_2 increases from 33% to 89%, C-(A)-S-H forms along with the C_2ASH_8. This is accompanied by an increase in CH consumed, but a decrease in the Q. Above a 89% SiO_2 content in the SCM, only C-(A)-S-H is formed. An SCM with 89%SiO_2+11%Al_2O_3 is predicted to release the least Q. Note how this minimum predicted Q occurs at 33%SiO_2+67%Al_2O_3 when the CSHQ model is used and at 89%SiO_2+11%Al_2O_3 when the CNASH model is used. This is due to the lower enthalpies of formation of the Al-rich C-(A)-S-H phases in the CNASH model when compared to the C-S-H phases in the CSHQ model. It is also observed that between 33% SiO_2 and 89% SiO_2, the C/S and the A/S of the C-(A)-S-H predicted to form are uniformly C/S=0.8 and A/S=0.06. From a 89% SiO_2 content to 100% SiO_2, the C/S decreases from 0.8 to 0.7, and the A/S decreases from 0.06 to 0. This is accompanied by an increase in the Q and CH consumed. Note that the Q and the CH consumed at 100% SiO_2 predicted by the CNASH model are higher than that predicted by the

CSHQ model. This is because the upper C/S limit of the CNASH model is C/S=1.5, and the C/S of the C-S-H formed in the PRT when SiO_2 is tested is closer to C/S=1.7 (33) (the limit for the CSHQ model is C/S=2.25, so the CSHQ model can predict the C-S-H that forms more accurately).

Figure A-1(b) shows a PRT style plot with the reactivity lines for the different combinations of SiO_2+Al_2O_3 tested in the PRT. Despite these small differences in the Q and CH consumed between the CSHQ model and CNASH model explained in the previous paragraph, from this figure it is clear that the CSHQ model is sufficient to calculate the DOR* from the PRT. The difference in predicted Q for high-Al SCMs (where C-(A)-S-H is expected to form) is under 5%. Additionally, data from the literature indicates that the predictions from the CNASH model are unsuitable for low-Al SCMs or in high-Al SCMs when CH is present in significant quantities (75-77).

REFERENCES

74. Kulik, D. A., "Improving the Structural Consistency of CSH Solid Solution Thermodynamic Models," Cement and Concrete Research, V. 41, No. 5, 2011, pp. 477-495. doi: 10.1016/j.cemconres.2011.01.012

75. Myers, R. J.; Bernal, S. A.; and Provis, J. L., "A Thermodynamic Model for C-(N-)A-S-H Gel: CNASH_ss. Derivation and Validation," Cement and Concrete Research, V. 66, 2014, pp. 27-47. doi: 10.1016/j.cemconres.2014.07.005

76. Myers, R. J.; Lothenbach, B.; Bernal, S. A.; and Provis, J. L., "Thermodynamic Modelling of Alkali-Activated Slag Cements," Applied Geochemistry, V. 61, 2015, pp. 233-247. doi: 10.1016/j.apgeochem.2015.06.006

77. Lothenbach, B., "Question about CSHQ vs. CNASH Models," personal communication sent to B. Isgor, 2020.

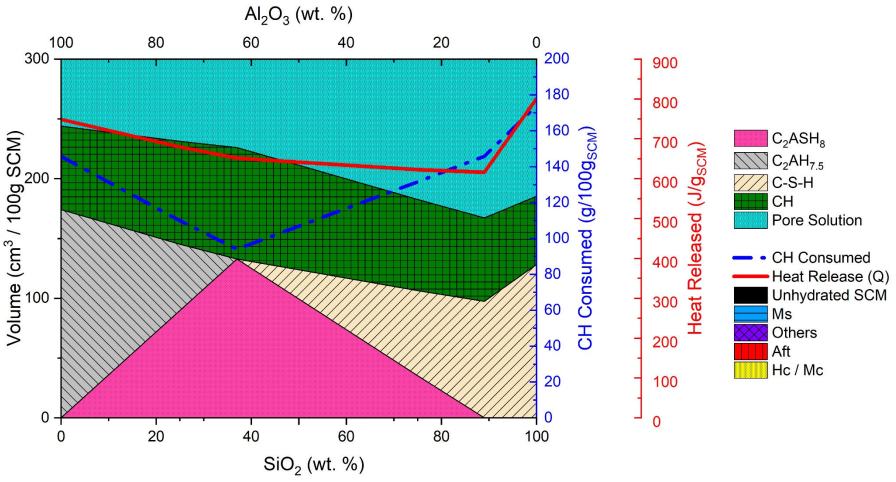

(a)

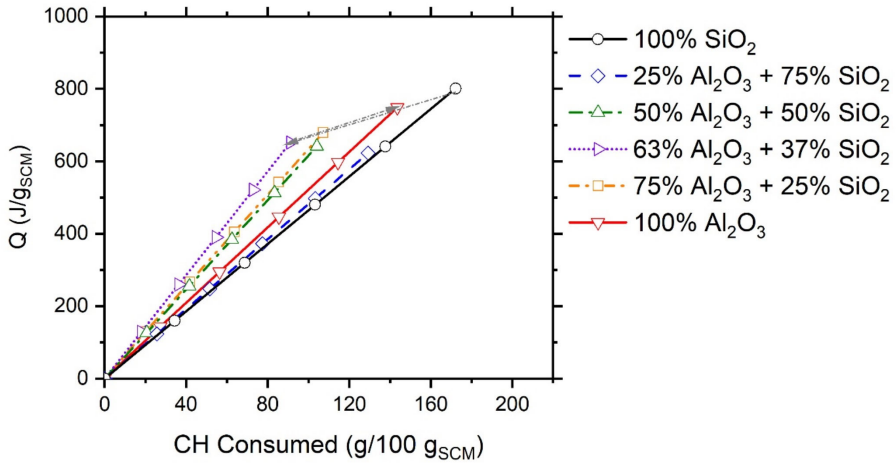

(b)

Figure A-1. (a) Phases that are predicted to form when the CNASH model is used as the proportion of SiO_2 to Al_2O_3 is varied; (b) Theoretical reactivity lines as predicted by the CNASH model: values of Q vs. CH consumed for ideal SCMs containing varying proportions of SiO_2 and Al_2O_3.